Journal of Materials Chemistry B

RSC Publishing

PAPER

View Article Online
View Journal | View Issue

Cite this: J. Mater. Chem. B, 2013, 1, 4956

Highly dispersible PEGylated graphene/Au composites as gene delivery vector and potential cancer therapeutic agent†

Fang-Fang Cheng,[a] Wei Chen,[b] Li-Hui Hu,[a] Gang Chen,[a] Hai-Tao Miao,[a] Chenzhong Li[c] and Jun-Jie Zhu*[a]

Received 9th May 2013
Accepted 22nd July 2013

DOI: 10.1039/c3tb20656d

www.rsc.org/MaterialsB

Graphene/Au composites with a high positive charge, which is advantageous for the binding and condensation of negatively charged siRNA, are synthesized *via* an *in situ* reduction method, using PEI as a reductant and protective reagent. Owing to the sufficient amounts of amino groups, PEI-grafted graphene/Au composites can be further modified with methoxyl-PEG to acquire low cytotoxicity, novel blood compatibility, and optimal dispersibility in physiological environments. The obtained PEGylated PEI-grafted graphene/Au composites (PPGA) allow efficient loading of siRNA, forming PPGA/siRNA complexes to transport into HL-60 cells and downregulated anti-apoptosis Bcl-2 protein, indicating PPGA is a suitable platform for gene delivery. Moreover, PPGA display an enhanced photothermal response with respect to PPG under NIR laser irradiation, suggesting that PPGA can be used as an efficient photothermal agent.

1 Introduction

siRNA, which is composed of 19–23 nucleotide (nt) double-stranded RNA (dsRNA) segments, has emerged as a potential therapeutic strategy for many diseases *via* sequence-specific gene silencing, named RNA interference (RNAi), whereby double-stranded small interfering RNA (siRNA) can be incorporated into RNA-induced silencing complexes (RISC) and suppress the expression of pathogenic proteins through the degradation of the target messenger RNA (mRNA).[1–3] To our knowledge, naked siRNA cannot be transported through the cell membrane freely,[4,5] thus various delivery systems have been developed to help active siRNA to access the cytoplasm of the target cell. Usually, delivery systems can typically be categorized into viral and non-viral vectors.[6] Viral vectors provide highly efficient delivery but induce immune response.[7] Therefore great effort is devoted to exploiting non-viral delivery systems based on such material platforms as lipids,[8,9] polymers,[10–12] and inorganic nanoparticles,[13–15] *etc.* due to their safety, non-immunogenicity and ease of manufacture.[16]

Graphene, well known for its unique electrical, optical and mechanical properities,[17–19] has attracted a lot of research interest in its biological application, including biosensors,[20,21] drug delivery,[22–25] cellular imaging,[26] and photothermal therapy.[27–29] Recently, it has been reported that graphene and graphene oxide are successfully used as anticancer drug delivery systems for cancer therapy because of low cytotoxicity and high drug loading efficiency, demonstrating their novel properties as nanocarriers for drugs, siRNA and gene delivery.[22,24] Furthermore, graphene oxide was proven to be an outstanding fluorescence quencher to detect nucleic acid because GO selectively adsorbs nonstructured and single-stranded DNA (ssDNA), but desorbs double-stranded (dsDNA) or well-folded structures so that it is difficult for graphene oxide to immobilize double-stranded siRNA which largely limits GO as a siRNA vector.[30] Zhang *et al.* and Liu *et al.* employed PEI to conjugate with GO through amide reaction or electrostatic interaction and then load siRNA *via* electrostatic absorption.[31,32] Unfortunately, PEI-coated GO exhibited significant toxicity because of the high charge density of PEI.[33,34] It is of crucial importance to find approaches that reduce PEI's toxicity and simultaneously preserve its gene delivery performance. PEG has been extensively used to increase stability in physiological conditions, reduce toxicity and lower immunogenicity as well as prolong circulation time in blood.[35–37]

Herein, graphene/Au composites of high positive charge are synthesized *via* an *in situ* reduction method in the presence of PEI, and then further functionalized with mPEG through an amidation reaction between the amino groups of PGA and the NHS active ester groups of mPEG-SPA. The obtained PEGylated

[a]State Key Lab of Analytical Chemistry for Life Science, School of Chemistry and Chemical Engineering, Nanjing University, Nanjing, 210093, P.R.China. E-mail: jjzhu@nju.edu.cn; Fax: +86-25-8359-4976; Tel: +86-25-8359-4976

[b]State Key Laboratory of Pharmaceutical Biotechnology, Department of Biochemistry, Nanjing University, Nanjing 210093, China

[c]Department of Biomedical Engineering, Florida International University, 10555 W. Flagler St., Miami, Florida 33174, USA

† Electronic supplementary information (ESI) available. See DOI: 10.1039/c3tb20656d

PEI-grafted graphene/Au composites (PPGA) exhibited high water dispersibility, low cytotoxicity and excellent blood compatibility which was an obstacle for gene transfection *in vivo*. PPGA/siRNA complexes provided a high transfection efficiency, similar to Lipofectamine 2000. Meanwhile, PPGA perform a sensitive photothermal effect, demonstrating that PPGA could be a promising nonviral vector and photothermal agent.

2 Experimental section

2.1 Materials

Graphite powder (KS-10) and branched polyethyleneimine (PEI, 25 KDa) were purchased from Sigma-Aldrich (Shanghai, China). Anti-Bcl-2 and anti-tubulin β antibodies were bought from Beijing Biosynthesis Biotecnology Co., Ltd (Beijing, China). Chloroauric acid ($HAuCl_4$) was obtained from Shanghai Reagent Company (Shanghai, China). WST, agarose, diethyl pyrocarbonate (DEPC), BCA protein assay kit and cell lysis buffer were purchased from Beyotime Institute of Biotechnology (Nantong, China). Lipofectamine 2000 was purchased from Invitrogen (NY, USA). Methoxy polyethylene glycol succinimidyl propionate (mPEG-SPA, 2 KDa) was bought from Shanghai Yare Biotech, Inc. (Shanghai, China). Dulbecco's modified Eagle's medium (DMEM), fetal bovine serum (FBS) and penicillin–streptomycin solution were purchased from HyClone Laboratories, Inc. (USA). Opti-modified Eagle's medium (Opti-MEM) was purchased from Gibco (Grand Island, NY). siRNA oligonucleotides were Bcl-2-targeted siRNAs, obtained from Shanghai Genepharma Co., Ltd. The sequences included: sense strand, 5′-GUACA UCCAUUAUAAGCUGdtdt-3′; anti-sense strand, 5′-CAGCUUA UAAUGGAUCdtdt-3′. FAM-labeled siRNA was obtained by adding fluorescein amidite (FAM) at the 5′-end of the sense strand (5′-FAM-GUACAUCCAUUAUAAGCUGdtdt-3′). Water was purified with a Millipore Milli-Q water system to achieve a final resistance of 18.2 MΩ. All solutions were prepared using ultrapure water treated with 0.1% DEPC.

2.2 Synthesis of PEI-RGO/Au composite (PGA)

GO was prepared by a modified Hummers method using graphite powder as starting material.[37] The obtained GO was sonicated in an ice bath using a probe-type sonicator under a power of 40 W for 4 h to obtain a transparent homogeneous solution and filtered through a PTFE membrane (0.45 mm pore size). PEI modified graphene/Au composites (PGA) were prepared according to the following procedure. In brief, the mixture containing GO (10 mL, 0.05 mg mL^{-1}) was stirred in PEI (10 mL, 2 mg mL^{-1}) for 10 min and sonicated for 30 min. The mixture was centrifuged at 22 000 rpm for 30 min to obtain PEI-grafted GO (PGO). $HAuCl_4$ (1%, 100 μL) was added into 20 mL 0.025 mg mL^{-1} PGO and sonicated for 30 min. 20 mL PEI (2 mg mL^{-1}) were then added and reacted at 90 °C for 6 h in a round bottomed flask. The as-prepared PEI-grafted Graphene/Au (PGA) was centrifuged at 22 000 rpm for 30 min, washed several times with deionized water, and then suspended in water for further use.

2.3 Synthesis of mPEG-PGA (PPGA)

0.01 mL, 0.05 mL, 0.1 mL, 0.2 mL, 0.5 mL 20 mg mL^{-1} of mPEG-SPA was added into a solution of PGA (0.8 mg mL^{-1}, 1 mL) and ultrasonicated for 10 min, respectively. The reaction solution was vibrated overnight at room temperature. The resulting PEGylated PGA (PPGA) was purified by centrifugation at 22 000 rpm for 30 min and washed three times with pure water to remove residual mPEG-SPA.

2.4 Preparation of PPGA/siRNA complexes and agarose gel retardation assay

PPGA/siRNA complexes were prepared *via* electrostatic interactions. An agarose gel retardation assay was used to determine the siRNA binding to PPGA. A 10 μL aliquot of 2 μM siRNA was mixed with 10 μL of PPGA with different concentrations in aqueous solution to obtain particles/nucleic acid mass ratios of 150 : 4, 100 : 4, 75 : 4, 37.5 : 4, 18.75 : 4, 15 : 4, 10 : 4, 5 : 4, 0 : 40 for 30 min. Then 10 μL of the PPGA/siRNA solution were mixed with 2 μL of 6× loading buffer and electrophoresed in 1.5% agarose gel containing 0.5 μg mL^{-1} ethidium bromide (EB) in Tris-acetate–EDTA buffer (TAE, pH 8.0) at 100 V for 40 min. Naked siRNA was used as a control. Nucleic acid bands were visualized by UV irradiation (254 nm), and the photographs were captured in a Bio-Rad imaging system (Hercules, CA).

2.5 Cell culture and cytotoxicity assays

Human promyelocytic leukemia cells (HL-60) were cultured in Dulbecco's Modified Eagle Medium (DMEM) supplemented with 10% fetal bovine serum (FBS) in a fully humidified atmosphere at 37 °C with 5% CO_2. The cell viability of HL-60 cells was tested with WST-1 according to the manufacturer's instructions. WST-1 assay was based on the cleavage of the tetrazolium salt to formazan by cellular mitochondrial dehydrogenase. Bioreduction of WST-1 produces a water-soluble formazan, which eliminates the need for an additional solubilization step. The amount of formazan produced is directly proportional to the number of living cells. For this procedure, HL-60 cells were seeded in 96-well plates at a density of 1×10^4 cells per well and maintained in 100 μL culture medium containing PPGA at 0 μg mL^{-1}, 10 μg mL^{-1}, 20 μg mL^{-1}, 40 μg mL^{-1}, 60 μg mL^{-1}, 80 μg mL^{-1} and 100 μg mL^{-1} for 24 h and 48 h, respectively. After incubation, 10 μL of WST-1 reagent were added to all cell culture media and incubated for 4 h at 37 °C. The plates were then read by a scanning multiwall spectrophotometer by measuring the absorbance of the dye with a wavelength of 450 nm. All measurements were taken in triplicate from three independent experiments.

2.6 Cell transfection and cellular uptake of PPGA/siRNA complexes

Cell transfection was performed following a standard protocol. HL-60 was suspended in FBS free-DMEM medium at a concentration of 1×10^5 cells per mL. 2 mL of cell suspension were placed in each well of a 6-well plate and then transfected

with 1 μg siRNA formulated in PPGA or Lipofectamine 2000 in 0.5 mL Opti-MEM medium at 37 °C for 4 h. Then 250 μL FBS were added into FBS free-DMEM medium and the cells continued to be cultured for the required times.

To investigate the cellular uptake of PPGA/siRNA, the fluorescence of FAM-labeled siRNA after cellular uptake was monitored by confocal laser scanning microscopy (CLSM). Cells were incubated with PPGA/FAM-siRNA containing 1 μg of siRNA. After 24 h, the distribution of the nucleic acids was examined and recorded in living cells by CLSM excited at 488 nm, and emitted at 522 nm for FAM. The images were analyzed using Leica CLSM software. Lipofectamine 2000/FAM-siRNA was used as a positive control.

2.7 Hemolysis assay and erythrocyte aggregation

EDTA–anticoagulated blood was centrifuged for 5 min at a speed of 1000 rpm. The serum fraction was removed and erythrocytes (RBC) were washed with physiological saline solution three times. The final suspension was diluted 1 : 10 with 100 mM phosphate buffer (pH 7.4). PPGA with different concentrations (100 μL) were added to the erythrocyte suspension of 1 mL. Pure phosphate buffered saline (PBS) was used as a negative control and Triton X-100 (1%, *v*/*v*) was used as a positive control. All samples were incubated under gentle agitation for 2 h at 37 °C and centrifuged at 1000 rpm for 5 min. The absorbance of the supernatant was measured for release of haemoglobin at 540 nm.[38,39] The percentage of haemolysis was calculated as follows:

$$\text{Haemolysis}\% = (\text{absorbance of test sample} - \text{absorbance of negative control})/(\text{absorbance of positive control} - \text{absorbance of negative control}) \times 100\%$$

For erythrocyte aggregation, pure PBS was used as a negative control, PEI served as a positive control. 200 μL of 500 μg mL^{-1} PPAG were incubated with 800 μL erythrocytes at 37 °C for 2 h. Each sample was placed on glass slides and monitored for erythrocyte aggregation with a light microscope.

2.8 Western blot assay

Total proteins were extracted from PPGA/siRNA-transfected or Lipofectamine/siRNA-transfected cells. Cells were lysed in cell lysis buffer and lysates were then clarified by centrifugation at 12 000 rpm for 10 min at 4 °C to separate the soluble from the pellet insoluble fraction. The proteins were quantified with BCA protein assay. The extract was then removed and mixed with loading. Proteins were boiled, resolved in SDS-polyacrylamide gel, transferred to polyvinylidene difluoride membranes (PVDF), blocked with blocking buffer (5% skimmed milk in PBS with 0.02% Tween-20) and incubated with the indicated rabbit primary polyclonal anti-Bcl-2 and anti-tubulin β antibodies at room temperature for 2 hours. Blots were washed three times for 5 min each in PBST (PBS with 0.02% Tween-20), and then incubated with HRP-conjugated secondary antibodies in blocking buffer and ECL reagent. Following three washes with PBST, the blots were visualized by the Bioshine ChemiQ.

2.9 Characterization

UV-vis spectra were recorded on a UV-3600 spectrophotometer (Shimadzu, Kyoto, Japan). Transmission electron micrographs (TEM) were measured on a JEOLJEM 200CX transmission electron microscope, using an accelerating voltage of 200 kV. Confocal laser scanning microscopy (CLSM) studies were performed using a Leica TCS SP5 microscope (Germany) with excitation at 488 nm. Dynamic light scattering (DLS) was conducted using a laser diffraction particle size analyzer (Mastersizer, Malvern Instruments, USA). Zeta Potential was tested on a nano-z zeta potential analyzer (Malvern Instruments, USA). WST assay was recorded at 450 nm using a Bio-Rad 680 microplate reader.

3 Results and discussion

3.1 Preparation and characterization of PPGA

The PEGylated PEI-modified graphene/Au composites (PPGA) were synthesized as shown in Fig. 1. Firstly, PEI-coated graphene oxide (PGO) was obtained *via* electrostatic interaction and then $AuCl_4^-$ was anchored onto the surface of PGO. PEI-modified graphene/Au composites (PGA) were synthesized through one-step hydrothermal method under refluxing at 90 °C for 6 h in the presence of PEI which was used as both

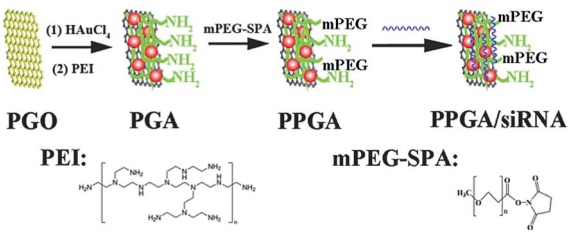

Fig. 1 Schematic illustration of the synthesis process of PPGA and the binding of siRNA.

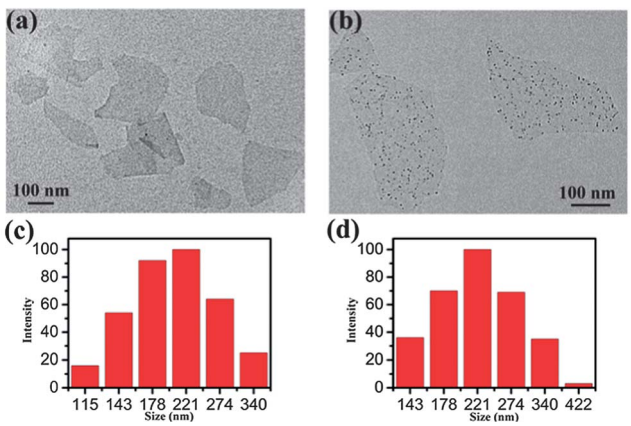

Fig. 2 Transmission electron microscopy images of GO (a) and PGA (b). Size distribution of GO (c) and PGA (d) by dynamic light scattering measurement.

reductant and protective reagent. To improve the colloidal stability of PGA in H_2O or phosphate buffered saline (PBS) solution, mPEG-SPA was introduced *via* an amidation reaction between the amino groups of PGA and the NHS active ester groups of mPEG-SPA. Finally, the prepared highly dispersible PPGA was used to delivery siRNA.

To characterize the PGA, TEM, DLS and UV-vis were performed. Compared to Fig. 2a, it is observed that Au nanoparticles with a diameter of about 10 nm deposit on the graphene sheets as shown in Fig. 2b. Moreover, almost no AuNPs are observed outside of graphene sheets, indicating that AuNPs combined well with graphene. Dynamic Light Scattering was performed to measure the hydrodynamic diameter of PGA complexes. As shown in Fig. 2c and d, the size of PGA is not significantly different from GO, ranging from 100 to 400 nm, demonstrating that PGA maintains an excellent dispersibility and does not exhibit aggregation, as well as PPGA and PPGA/siRNA (see Fig. S1 in the ESI†).

The aqueous dispersions of the samples were further characterized by the UV-vis spectra. The UV-vis spectra of GO show a strong band centered at 223 nm (Fig. 3a), which corresponds to the π–π^* transition of aromatic C–C bonds. After the reduction, the peak at 223 nm red shifted to 258 nm, indicating partial restoration of the π-conjugation structure of the graphene nanosheets. The absorption peaked at 519 nm exhibiting a well-defined excitation band of AuNPs, and the color of GO changed from brown to black after the reaction with PEI as the inset shows, indicating the successful synthesis of PGA as well.

To further improve the stability of PEI-grafted graphene/Au, mPEG-SPA was added to prepare PEGylated PEI-grafted graphene/Au. PEG can help eliminate phagocyte capture, provide better serum stability and extend blood circulation with low toxicity.[40] The effect of PEGylation on the charge of formed composites was investigated since surface charge is an important parameter for siRNA delivery systems. mPEG-SPA was added to the PEI-RGO/Au at different PGA/mPEG-SPA weight ratios. In Fig. 3b, the zeta potential of PGA was about 49.53 ± 1.63 mV in water. After PEGylation, the zeta potential of mPEG-PEI-graphene/Au decreased with the increasing volume of mPEG-SPA. The reason is that the NH_2 groups of PGA partly reduce because of the reaction between PGA and mPEG-SPA, suggesting mPEG-SPA is successfully conjugated with PGA. We chose the PPGA modified by 50 μL mPEG-SPA to perform the following work, because it has enough positive charge to catch siRNA as well as good stability in salt solution.

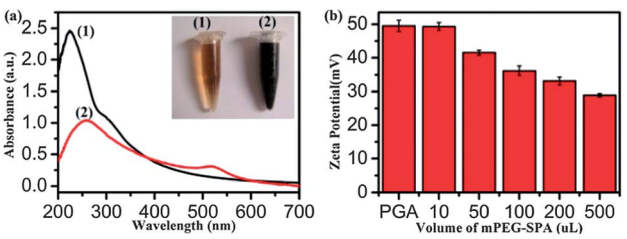

Fig. 3 (a) UV-vis absorbance spectra of GO (1) and PGA (2) solutions. The inset shows the photos of GO and PGA solutions. (b) Zeta potential of PGA reacted with different volumes of mPEG-SPA (20 mg mL^{-1}).

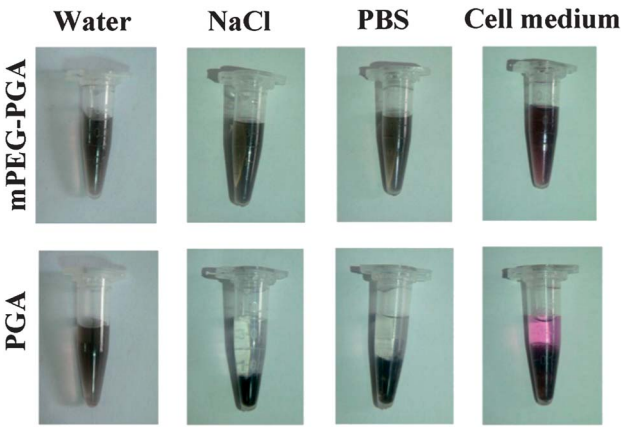

Fig. 4 Photos of PGA and PPGA in different solutions as indicated. PGA aggregated in the presence of salts and precipitated in saline, RPMI-1640 cell medium containing 10% fetal bovine serum while PPGA did not show this phenomenon.

The long-term stability of PPGA was further evaluated by suspending PPGA in physiological saline solution, PBS solution (pH 7.4) and culture media containing 10% FBS. As shown in Fig. 4, PGA was aggregated in physiological saline solution, PBS solution (pH 7.4) and culture media containing 10% FBS while PPGA while PPGA did not show the same phenomenon even after a week, demonstrating the excellent stability of PPGA in physiological environments which is necessary for gene transfection to cells, especially to suspension cells.

3.2 *In vitro* cytotoxicity and blood compatibility

One of the major obstacles to effective siRNA delivery is the cytotoxicity of non-viral vectors. In general, siRNA vectors are often associated with significant cytotoxic effects, due to their electrostatic interactions with negatively charged glycocalyx on cell membranes. Therefore, it is important to evaluate the cytotoxicity of PPGA when used as siRNA delivery carriers. Fig. 5a shows cell viability obtained from PPGA. The cell viability of PPGA was very low (nearly 38%) at the concentration of 100 μg mL^{-1} after 24 h. With the decreasing concentration of PPGA, the cell viability increased. The cell viability of PPGA reached 95% when the concentration of PPGA was below 20 μg mL^{-1}. The IC_{50} value for PPGA is about 68.7 μg mL^{-1}, higher than PEI-GO,[29] demonstrating that cytotoxicity of PPGA is lower than PEI-GO. In addition, the cell viability is time-dependent at high concentrations, but no significant difference was observed at low concentration, by comparing the cell viability of 24 h with that of 48 h. Therefore, PPGA at concentrations below 20 μg mL^{-1} can be used for siRNA delivery.

Because leukemia cells usually exist in blood, additional cytotoxicity assays were performed to analyze the effects of PPGA on haemolysis and aggregation of erythrocytes. Tests for excellent blood compatibility of the materials are necessary to determine if a delivery will be toxic when used *in vivo* even if no cytotoxicity is shown *in vitro*.[38] The hemolysis effect of the samples was quantitatively determined by measuring the absorbance of the supernatant at 541 nm (band of hemoglobin) using UV-vis spectroscopy as shown in Fig. 5b. As shown in

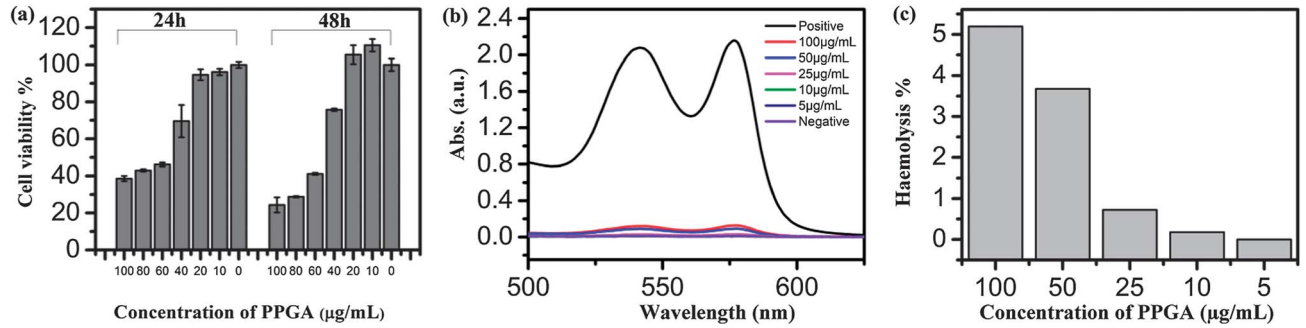

Fig. 5 (a) *In vitro* cell toxicity experiments. Relative viabilities of HL-60 cells after being incubated with various concentrations of PPGA for 24 h and 48 h. $p < 0.05$. (b) The UV-vis absorption spectra to detect hemoglobin in the supernatant of PPGA suspensions at different concentrations in PBS. Triton X-100 and PBS solution are used as the positive and negative controls, respectively. (c) Haemolysis percentage of PPGA at different concentrations.

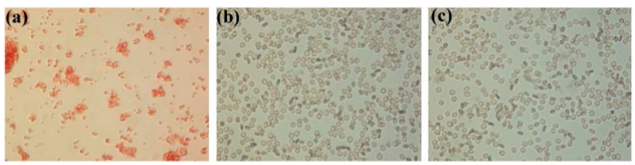

Fig. 6 Evaluation of erythrocytes aggregation treated with various samples: (a) Positive control (PEI), (b) PPGA, (c) negative control (PBS).

Fig. 5c, the hemolytic activity of PPGA was less than 6% even at the highest concentration of 100 μg mL^{-1}, indicating that PPGA have negligible hemolytic activity.

Following treatment with PBS, PPGA and PEI, erythrocytes were examined under a light microscope (Fig. 6). Treatment with PEI (Fig. 6a) resulted in the most aggregation, while treatment with PPGA (Fig. 6b) caused neither aggregation nor morphological deformity, similar to the negative control (Fig. 6c). Overall, the results indicated that the synthesized PPGA has low cytotoxic and shows tremendous advantages in safety in further applications for siRNA delivery, compared with PEI, a commercial transfection agent.

3.3 Characterization of PPGA/siRNA complexes

PPGA/siRNA complexes were obtained by electrostatic interaction as shown in Fig. 1. To investigate the loading capability of PPGA as siRNA carriers, agarose gel electrophoresis was performed and the results are shown in Fig. 7. 1 μg of siRNA was mixed with PPGA vectors of different masses in aqueous solution. It can be seen that the mobility of siRNA was not completely retarded until the PPGA/siRNA mass ratio increased to 75 : 4. Previous studies showed that PEI-GO could bind pDNA completely at mass raito > 1.[30] Therefore, the binding of siRNA was more difficult than for pDNA because of the rigid rod conformation of siRNA. On the other hand, the modification of mPEG can reduce nonspecific absorption of siRNA.

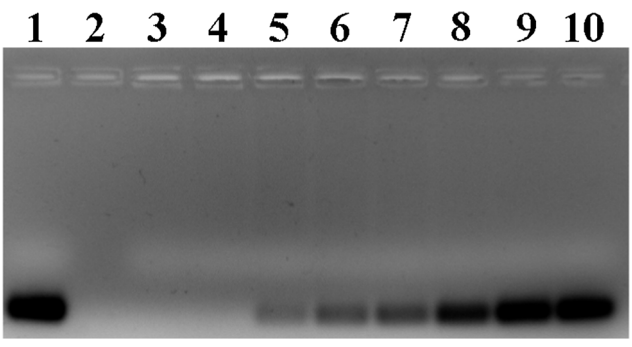

Fig. 7 Electrophoresis patterns of PPGA/siRNA complexes. Lane 1: pure siRNA ladder; lanes 2–10 represent the complexes with mass ratios (PPGA/siRNA) of 150 : 4, 100 : 4, 75 : 4, 37.5 : 4, 18.75 : 4, 15 : 4, 10 : 4, 5 : 4, 0 : 40, respectively.

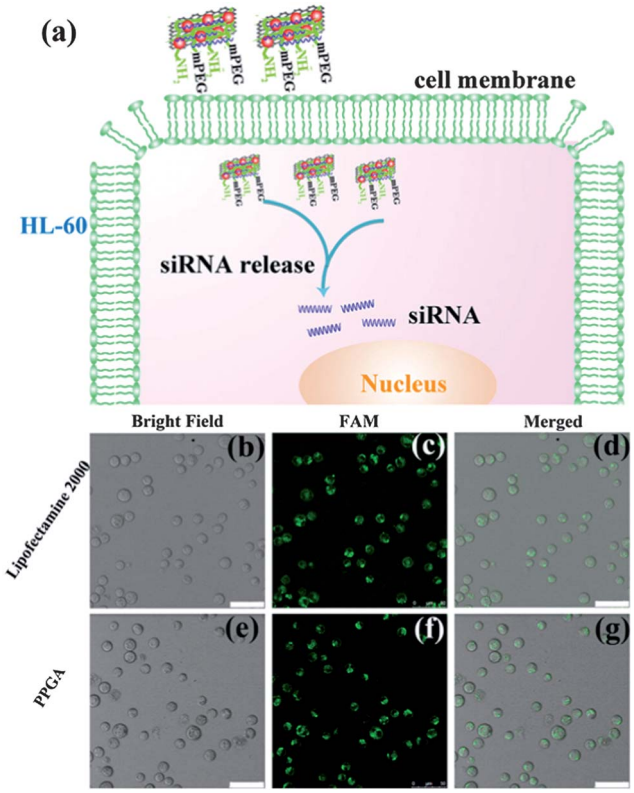

Fig. 8 Schematic illustration of positively charged PPGA binding with siRNA for intercellular delivery (a) and confocal laser scanning microscopy (CLSM) images of HL-60 cells incubated with Lipofectamine 2000/FAM labeled-siRNA (b–d) or PPGA/FAM labeled-siRNA (e–g) for 24 h. Scale bars correspond to 50 μm in all the images.

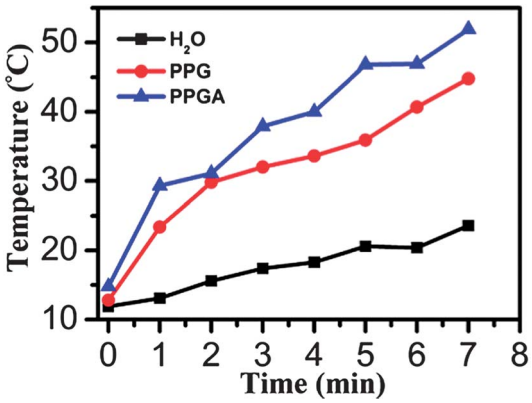

Fig. 9 Photothermal heating curves of PEGylated PEI-modified graphene (PPG) and PPGA solutions (0.25 mg mL^{-2}) under 808 nm laser irradiation at a power density of 2 W cm^{-2} for 7 min.

PPGA/siRNA at mass ratio of 100 : 4 was chosen in the following work. At this mass ratio, the concentration of PPGA was about 10 μg mL^{-1}, within the safe concentration range.

3.4 Cellular uptake of PPGA/siRNA

In achieving efficient transfection with siRNA, the delivery of siRNA across cell membrane is a key point. Endocytosis is the main mechanism by which nanoparticles or polymers enter living cells.[41] The delivery carriers need to cross the cell membranes, internalize through endocytosis and then release siRNA from the endosomes/lysosomes into the cytoplasm as shown in Fig. 8a. FAM-labeled siRNA was used as an indicator to enable the internalization and intracellular distribution of complexes in HL-60 cells to be visualized. *In vitro* siRNA delivery efficiency was performed by confocal laser scanning microscopy. Nucleic acids/polycations aggregation can interact with the membrane *via* hydrophobic and electrostatic interactions and exhibit endosomal escape *via* the "proton sponge effect" due to protonated amino groups of PEI.[6,40,42] In Fig. 9b–g, clear green fluorescence of PPGA/FAM-siRNA group and Lipofectamine 2000/FAM-siRNA was exclusively observed in the cytoplasm after 24 h transfection demonstrating that not only Lipofectamine 2000 but also PPGA showed excellent intracellular delivery. Three-dimensional images of entire cells after internalization of the PPGA/FAM-siRNA complex confirmed the presence of the complex inside cells as well (see Fig. S2 in the ESI†). The fluorescence intensity of siRNA in cells incubated with PPGA/FAM-siRNA group was slightly higher than that achieved by Lipofectamine 2000/FAM-siRNA complexes (see Fig. S3 in the ESI†). The reason is likely that graphene can protect the gene cargos against nuclease digestion or SSB interaction during prolonged transport.[43,44] In addition, the knockdown efficiency of the Bcl-2 protein expression level by PPGA/siRNA was studied. Bcl-2 protein was down regulated after cell seeded with PPGA/siRNA as well as Lipofectamine 2000/siRNA (see Fig. S4 in the ESI†). The above results thus demonstrate that PPGA is a safe and efficient alternative vector for siRNA delivery.

3.5 Photothermal effect of PPGA

In recent years, many graphene/metal nanoparticles composites have been under investigation for photothermal therapy (PTT) treatment of cancer, such as graphene/Fe_3O_4, graphene/Cu_2O, *etc.*[27,28] Herein, the photothermal effect of PPGA induced by the NIR absorption was also evaluated. When exposed to an 808 nm NIR laser at a power density of 2 W cm^{-2}, the temperature of PPGA solution remarkably increased from about 14.8 °C to 51.9 °C after 7 min irradiation, higher than the temperature change of water and PEGylated PEI-modified Graphene (PPG) under the same irradiation conditions. The reason is likely that graphene is able to convert light to heat for PTT and meanwhile the heat generating capacity of PPGA is higher than PPG, which is attributed to the presence of Au nanoparticles.[45,46] To evaluate the photothermal capability of PPGA, the viability of cells incubated with PPGA under NIR laser irradiation was detected. The viability of cells incubated with PPGA is about 46.8%, lower than PPG of 61.0% (see Fig. S5 in the ESI†). In all, PPGA has the potential to be considered a thermal agent.

4 Conclusions

In conclusion, highly dispersible PEGylated PEI-grafted graphene/Au composites were prepared *via* an *in situ* reduction reaction, rather than hybridization of PEI–graphene and Au nanoparticles. The prepared PPGA remained stable in biological solution, had lower cytotoxicity in comparison with PEI-GO and exhibited excellent blood compatibility. At the optimal mass ratio of PPGA/siRNA, the transfection efficiency of PPGA is similar to Lipofectamine 2000, a proprietary formulation for the transfection of nucleic acids into eukaryotic cells. At the same time, PPGA displayed an enhanced photothermal effect because of Au nanoparticles under NIR light. These results demonstrated that PPGA would be a remarkable nonviral vector and photothermal agent.

Acknowledgements

We greatly appreciate the support of the National Basic Research Program of China (2011CB933502), and National Natural Science Foundation of China (Grants 21121091 and 21020102038). FF Cheng thanks the support by the program B for outstanding PhD candidates of Nanjing University.

Notes and references

1 S. Y. Duan, W. E. Yuan, F. Wu and T. Jin, *Angew. Chem., Int. Ed.*, 2012, **51**, 7938–7941.
2 S. M. Elbashir, J. Harborth, W. Lendeckel, A. Yalcin, K. Weber and T. Tuschl, *Nature*, 2001, **411**, 494–498.
3 H. Mok, O. Veiseh, C. Fang, F. M. Kievit, F. Y. Wang, J. O. Park and M. Q. Zhang, *Mol. Pharmaceutics*, 2010, **7**, 1930–1939.
4 D. Peer and J. Lieberman, *Gene Ther.*, 2011, **18**, 1127–1133.
5 D. S. Lin, Y. Y. Huang, Q. Jiang, W. D. Zhang, X. Y. Yue, S. T. Guo, P. Xiao, Q. Du, J. F. Xing, L. D. Deng, Z. C. Liang and A. J. Dong, *Biomaterials*, 2011, **32**, 8730–8742.

6 X. Li, Y. J. Chen, M. Q. Wang, Y. J. Ma, W. L. Xia and H. C. Gu, *Biomaterials*, 2013, **34**, 1391–1401.
7 W. J. Kim and S. W. Kim, *Pharm. Res.*, 2009, **26**, 657–666.
8 S. Biswas, P. P. Deshpande, G. Navarro, N. S. Dodwadkar and V. P. Torchilin, *Biomaterials*, 2013, **34**, 1289–1301.
9 C. L. Walsh, J. Nguyen, M. R. Tiffany and F. C. Szoka, *Bioconjugate Chem.*, 2013, **24**, 36–43.
10 Y. Zhang, M. Y. Zheng, T. Kissel and S. Agarwal, *Biomacromolecules*, 2012, **13**, 313–322.
11 C. B. He, L. C. Yin, C. Tang and C. H. Yin, *Biomaterials*, 2013, **34**, 2843–2854.
12 X. Z. Yang, S. Dou, Y. C. Wang, H. Y. Long, M. H. Xiong, C. Q. Mao, Y. D. Yao and J. Wang, *ACS Nano*, 2012, **6**, 4955–4965.
13 E. Crew, S. Rahman, A. Razzak-Jaffar, D. Mott, M. Kamundi, G. Yu, N. Tchah, J. Lee, M. Bellavia and C. J. Zhong, *Anal. Chem.*, 2011, **84**, 26–29.
14 J. Jung, A. Solanki, K. A. Memoli, K. i. Kamei, H. Kim, M. A. Drahl, L. J. Williams, H. R. Tseng and K. Lee, *Angew. Chem., Int. Ed.*, 2010, **49**, 103–107.
15 Y. M. Yang, F. Liu, X. G. Liu and B. Z. Xing, *Nanoscale*, 2013, **5**, 231–238.
16 Y. B. Shan, T. Luo, C. Peng, R. L. Sheng, A. Cao, X. Y. Cao, M. W. Shen, R. Guo, H. Tomás and X. Y. Shi, *Biomaterials*, 2012, **33**, 3025–3035.
17 H. L. Wang, Y. Yang, Y. Y. Liang, G. Y. Zheng, Y. G. Li, Y. Cui and H. J. Dai, *Energy Environ. Sci.*, 2012, **5**, 7931–7935.
18 G. Eda and M. Chhowalla, *Adv. Mater.*, 2010, **22**, 2392–2415.
19 Y. Chen, Y. Y. Shen, D. Sun, H. Y. Zhang, D. B. Tian, J. R. Zhang and J. J. Zhu, *Chem. Commun.*, 2011, **47**, 11733–11735.
20 H. F. Dong, L. Ding, F. Yan, H. X. Ji and H. X. Ju, *Biomaterials*, 2011, **32**, 3875–3882.
21 H. B. Wang, Q. Zhang, X. Chu, T. T. Chen, J. Ge and R. Q. Yu, *Angew. Chem., Int. Ed.*, 2011, **50**, 7065–7069.
22 Z. Liu, J. T. Robinson, X. Sun and H. J. Dai, *J. Am. Chem. Soc.*, 2008, **130**, 10876–10877.
23 X. J. Fan, G. Z. Jiao, W. Zhao, P. F. Jin and X. Li, *Nanoscale*, 2013, **5**, 1143–1152.
24 X. Y. Yang, X. Y. Zhang, Y. F. Ma, Y. Huang, Y. S. Wang and Y. S. Chen, *J. Mater. Chem.*, 2009, **19**, 2710–2714.
25 X. M. Sun, Z. Liu, K. Welsher, J. T. Robinson, A. Goodwin, S. Zaric and H. J. Dai, *Nano Res.*, 2008, **1**, 203–212.
26 C. S. Wang, J. Y. Li, C. Amatore, Y. Chen, H. Jiang and X. M. Wang, *Angew. Chem., Int. Ed.*, 2011, **50**, 11644–11648.
27 C. Y. Hou, H. C. Quan, Y. R. Duan, Q. H. Zhang, H. Z. Wang and Y. G. Li, *Nanoscale*, 2013, **5**, 1227–1232.
28 X. X. Ma, H. Q. Tao, K. Yang, L. Z. Feng, L. Cheng, X. Z. Shi, Y. G. Li, L. Guo and Z. Liu, *Nano Res.*, 2012, **5**, 199–212.
29 K. Yang, S. Zhang, G. X. Zhang, X. M. Sun, S. T. Lee and Z. Liu, *Nano Lett.*, 2010, **10**, 3318–3323.
30 L. M. Zhang, Z. X. Lu, Q. H. Zhao, J. Huang, H. Shen and Z. Zhang, *Small*, 2011, **7**, 460–464.
31 B. Chen, M. Liu, L. M. Zhang, J. Huang, J. L. Yao and Z. J. Zhang, *J. Mater. Chem.*, 2011, **21**, 7736–7741.
32 L. Z. Feng, S. Zhang and Z. Liu, *Nanoscale*, 2011, **3**, 1252–1257.
33 Y. Ping, C. D. Liu, G. P. Tang, J. S. Li, J. Li, W. T. Yang and F. J. Xu, *Adv. Funct. Mater.*, 2010, **20**, 3106–3116.
34 M. D. Shau, M. F. Shih, C. C. Lin, I. C. Chuang, W. C. Hung, W. E. Hennink and J. Y. Cherng, *Eur. J. Pharm. Sci.*, 2012, **46**, 522–526.
35 M. Zheng, D. Librizzi, A. Kılıç, Y. Liu, H. Renz, O. M. Merkel and T. Kissel, *Biomaterials*, 2012, **33**, 6551–6558.
36 X. Z. Yang, J. Z. Du, S. Dou, C. Q. Mao, H. Y. Long and J. Wang, *ACS Nano*, 2011, **6**, 771–781.
37 W. S. Hummers and R. E. Offeman, *J. Am. Chem. Soc.*, 1958, **80**, 1339–1339.
38 Z. X. Zhao, S. Y. Gao, J. C. Wang, C. J. Chen, E. Y. Zhao, W. J. Hou, Q. Feng, L. Y. Gao, X. Y. Liu and L. R. Zhang, *Biomaterials*, 2012, **33**, 6793–6807.
39 A. L. Lyncha, R. J. Chen and N. K. H. Slatera, *Biomaterials*, 2011, **32**, 4443–4449.
40 M. Malhotra, C. Tomaro-Duchesneau and S. Prakash, *Biomaterials*, 2013, **34**, 1270–1280.
41 C. S. Paulo, R. P. das Neves and L. S. Ferreira, *Nanotechnology*, 2011, **22**, 494002.
42 Z. J. Dai, T. Gjetting, M. A. Mattebjerg, C. Wu and T. L. Andresen, *Biomaterials*, 2011, **32**, 8626–8634.
43 L. Cui, X. Y. Lin, N. H. Lin, Y. L. Song, Z. Zhu, X. Chen and C. J. Yang, *Chem. Commun.*, 2012, **48**, 194–196.
44 Z. W. Tang, H. Wu, J. R. Cort, G. W. Buchko, Y. Y. Zhang, Y. Y. Shao, I. A. Aksay, J. Liu and Y. H. Lin, *Small*, 2010, **6**, 1205–1209.
45 I. H. El-Sayed, X. Huang and M. A. El-Sayed, *Cancer Lett.*, 2006, **239**, 129–135.
46 A. F. Zedan, S. Moussa, J. Terner, G. Atkinson and M. S. El-Shall, *ACS Nano*, 2012, **7**, 627–636.

